Characterization of Advanced Ceramic Materials Thin Films Deposited on Fe-C Substrate

COSTEL DOREL FLOREA[1], CORNELIU MUNTEANU[1], NICANOR CIMPOESU[1], IOAN GABRIEL SANDU[1,2], CONSTANTIN BACIU[1], COSTICA BEJINARIU[1]*

[1] Gheorghe Asachi Technical University of Iasi, Faculty of Materials Science and Engineering, 67 D. Mangeron Blvd., 700050, Iasi, Romania

[2] Romanian Inventors Forum, 3 Sf Petru Movila St., Bl. L11, Sc. A, III/3, 700089, Iasi, Romania

Complex ceramic superficial ceramic layers (Al_2O_3, SiO_2, YO, ZrO_2) were obtained by atmospheric plasma deposition, industrial wide application method, on a metal support Fe-C (FC 250). The substrate was sandblasted mechanically prior to depositing 6 successive layers of ceramic material. The obtained layers were analyzed structurally (scanning electron microscopy, SEM), chemical (spectroscopy of X-ray, EDAX) and mechanically (scratch tests) to characterize the new compound material obtained (thin layer-substrate). It was observed from the experimental results that there was a relationship between the state of the surface of the substrate and the adhesion of the ceramic layers to the metal surface.

Keywords: complex ceramic, plasma, SEM, EDAX, scratch

The friction between two dry surfaces moving relative to each other is known as Coulomb friction and even if it is a phenomenon that occurs several times a day friction forces can only be estimated from previous experience and experimental results. In the case of braking systems (for any type of vehicle using braking systems) the contact surfaces are often covered with different materials to result in a sliding process and are not just two metallic materials sliding on each other [1-5]. The metallic surface will be affected by abrasion, adhesion of compounds other than the base material, or deformation of the material during sliding through which metallic fragments of material and other particles will be created [6-8].

During the braking process, the materials of the plate and of the rotor disk are subject to severe stress and the behavior of these materials depends on the microstructure of the material and the nature of the chemical constituents. Changes in tribological and mechanical behavior depend largely on the nature and size of metal compounds that are generally quite complex metal systems [9-12]. The scientific understanding of the friction phenomenon has advanced much on the basis of experimental results, but the complicated nature of brake friction involving very high energies, very high temperatures, very high speeds and pressures makes this process an inexact yet based on knowledge and power the understanding of the specialists [13-19].

In order to obtain metallic brake discs used for consumer vehicles, low-cost materials such as FC 250 [20] are used. Vehicle speeds are steadily increasing and braking demands have increased greatly over the last decade. Meanwhile, various solutions are being sought to improve the braking characteristics of vehicles by replacing classical materials with higher alloys, different geometries of the brake discs, or deposition of thin layers with special properties [21, 22].

The method of plasma spray deposition in air uses gas jets with extremely high temperatures to melt the material. This jet is formed by heating the inert gases in the electric arc to the plasma state of the materials. Plasma temperature usually exceeds 15.000 K [23, 24]. The plasma deposition process is considered to be the most widespread method of all sputter deposition and has numerous applications at the industrial level as well. New research shows that the thin layer obtained has a high density (> 97%) than the theoretical and the oxygen content is below 400 ppm [24]. Plasma deposition can be performed in different media, such as vacuum, low pressure, inert gas or atmospheric plasma. To apply plasma spraying at industrial level, plasma spraying in the atmosphere is one of the greatest opportunities at this time. Throughout the world, the thermal deposition technology market is very diverse, with coverage in areas such as wear, thermal barriers, atmospheric corrosion protection, corrosion protection at high temperatures and oxidation control tolerances, moving parts, conductivity and electrical insulation, biomedicine, or dimensional restructuring [25-29].

This paper proposes a solution for improving the surface properties of a cast iron with industrial applications, FC 250, by depositing complex ceramic layers by thermal spraying into the air. The obtained layers were analyzed by electronic microscopy, spectrometric analysis and adhesion tests.

Experimental part

Thin ceramic layers (60 μm) were deposited on a cast iron substrate (FC 250) using the air spray method using SPRAYWIZARD 9MCE. The deposition material is a combination of yttrium oxide stabilized zirconia powders (80% ZrO_2/8% Y_2O_3 - Metco 204B-NS) and 20% alumina (Al_2O_3 - Metco 105SFP), wear resistance at temperature [30].

To increase the adhesion of the deposited complex layer it is necessary to prepare the surface by sandblasting. For this stage, the Rosler equipment was subjected to a dry powder sandblasting operation for the low roughness test and one with aluminum oxide (Al_2O_3) Fepa 40 (430 μm) for the higher rugged sample, both with a 3 bar pressure. A Bruker EDS detector (PB-ZAF mode) was used to determine the chemical composition and the surface state was analyzed using the SEM VegaTescan LMHII (SE detector, 30 kV) scanning electron microscopy [31-33]. Mechanical determinations were performed on a MTU (Universal

* email: costica.bejinariu@yahoo.com

Micro-Tribumer: a 150 mm programmable maximum track at a rate of 0.001 - 10 mm/s, a 1 µm decoder with a specific resolution of 100 nm) [34].

Results and discussions

Modification of the surface of the standard material by mechanical blasting

Athmospheric thermal spraying requires surface processing of the material through a blasting operation to increase the adhesion of the substrate to the substrate. Surface splicing can be accomplished by various chemical, physical or mechanical methods, depending on the results.

In order to cover with a ceramic material with high thermal insulation properties and with high wear resistance properties, the FC 250 cast iron base material with the surface shown in figures 1a and b was subsequently machined by mechanical sandblasting. The sanding yielded a fine surface (0.34 mm roughness) in which the lamellar graphite formations and their homogeneous distribution were also emphasized.

For the deposition, two samples were prepared by mechanical sandblasting with two types of different powder to modify the surface. Two samples, P1 and P2, were obtained with the following surface roughness values: P1: Ra - 2.47 µm and Rz - 18.37 µm respectively P2: Ra - 4.25 µm and Rz - 32.08 µm.

Figure 2 shows the state of the alloy surface FC 250 after sanding by 2D and 3D electronic microscopy. figure 2a and b show the state of the sample surface P1 by 2D microscopy at different amplification powers in figure 2c and d the state of the sample surface P2 by 2D microscopy at different amplification powers, figure 2e and f the 3D surface of the samples P1 and P2 respectively; and figure 2g and h variations in the light intensities characteristic of the two surfaces. A change in the surface is observed by forming and modifying the indentations left by the blasting material.

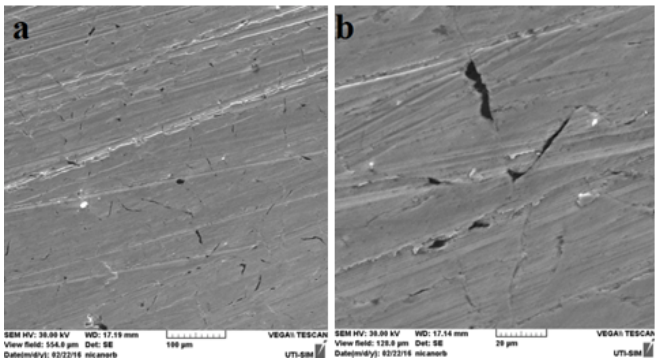

Fig. 1. Surface of FC 250 cast iron after sandblasting: a 500X and b. 1kX

Surface analysis revealed the formation of processing traces with mean depths of 5-10 µm (standard deviation of ± 1 µm) for sample P1 and 25-30 µm (standard deviation of ± 5 µm) for sample P2 (it was measured 50 sandblasting traces in 3D microscopy using the VegaTescan program).

After the samples were prepared by sandblasting, these were used as a substrate for making plasma jet deposits. The raw material deposited, a ceramic powder material, has a particle size of 35 µm. From the particle morphology of the deposition powder, at least two types of some rectangular particles and the other spheroidal particles, constituting this ceramic material, are observed and which are transformed into a compact layer after spraying.

From the qualitative chemical analysis carried out on the experimental powder we have identified the elements: O, Zr, Al, Y, C and Hf (fig. 3b). These belong to the oxides of the powder (Zr, Al and Y oxides) and Hf was identified due to the impregnation of zirconia powders (ZrO_2), a particular feature encountered in Zr-based powders used in industrial applications. Carbon appears only as a carbonation impurity element on which the experimental dusts were located.

Structural and chemical analysis of the surface of the metallic material after deposition of the ceramic layer

After the deposition of the complex ceramic material based on oxides of Al, Zr/Hf, and Y (generally zirconia and yttrium) by passing five times with the plasma jet, compact layers with estimated thicknesses of 50-60 µm, the thickness of the layer being an approximately linear function by the number of passes (1 - 12 µm). Figure 4 shows the states of the deposited layers.

The discontinuities of the deposited layer of any kind: pores, cracks, exfoliations, etc., are detrimental to the subsequent mechanical, chemical and physical properties. For these reasons, it is not recommended that plasma jet deposition be performed without prior macroscopic sample preparation to improve the adhesion of the deposited layer. On both surfaces there are microscopes. On P1 sample,

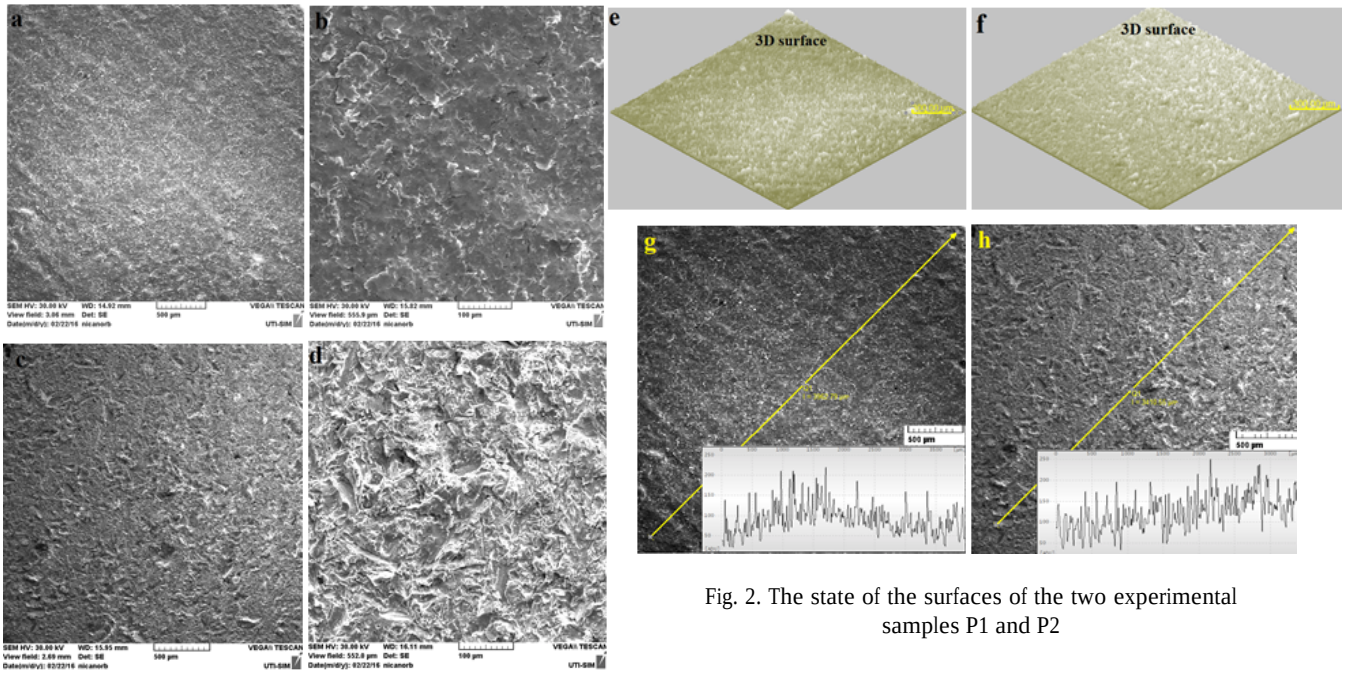

Fig. 2. The state of the surfaces of the two experimental samples P1 and P2

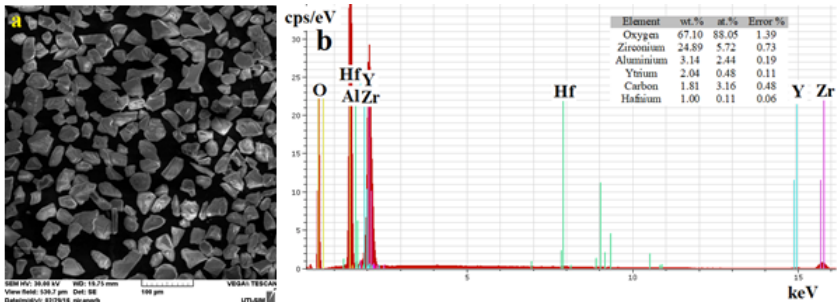

Fig. 3. Morphology of the particles making up the deposition material and the energy spectrum of the constituent elements of the proposed powder for castings

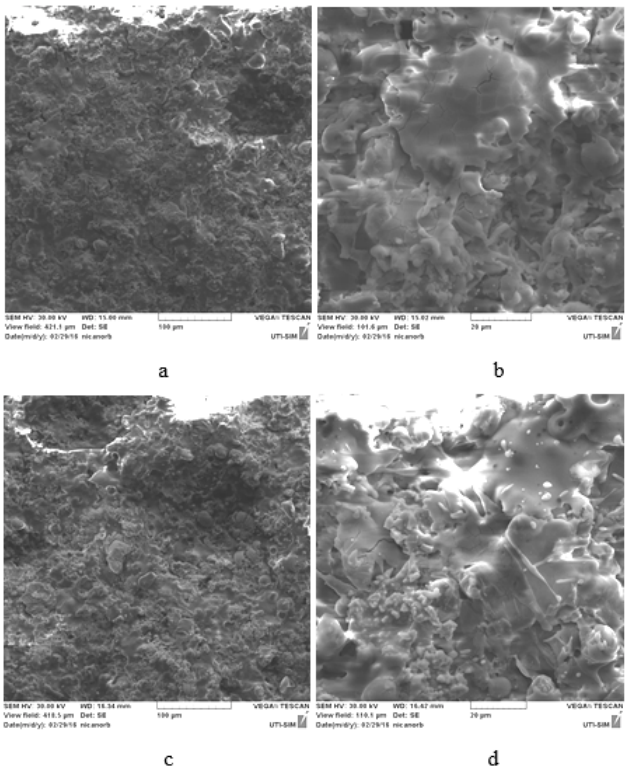

Fig. 4. SEM micrographs of deposited layers: a and b on sample P1 (500X or 2000X); c and d on sample P2 (500X or 2000X)

they are more numerous and have submicron thicknesses and lengths of 15-20 μm.

Figure 4c and d show the morphology of the layer deposited on the harder sandblasting, using alimin oxide particles, at two amplification powers. It is observed that a compact layer on the surface has been formed, without interruption or exfoliation, and which has local micro-cracks with micrometer lengths (fig. 4d). The cracks are on the surface, without penetrating the entire depth of the layer and are based on temperature differences between the last layer which is almost cooled and the last layer deposited at a very high temperature.

In both cases, the layer is generally composed of molten material areas (the powders previously analyzed) forming a compact ceramic mass by increasing the temperature at which they are brought (12,000°C).

Table 1 shows the chemical composition of the thermal spray coating. There is an increase in the percentage of aluminum oxides and a decrease in zirconium (zirconia) as compared to the percentage present in powders.

As far as the Y and Hf percentages are concerned, they have not undergone major changes, Hf following a decrease and confirming the loss of zirconium oxides during the deposition process. Compositions obtained for the layers deposited on the two samples P1 and P2 are closely related from the point of view of percentage confirmation of the stability of the deposition method even if it is applied at the industrial level.

Analysis of adhesion of superficial layers deposited by thermal spraying through scratch tests

To analyze the adhesion of superficial layers deposited on the FC 250 substrate, scratch tests, two tests for each sample, were performed on the two experimental samples P1 and P2.

From the characteristic variations of the forces applied to the layer it results that for the P2 sample a higher force is needed to perforate the deposited ceramic layer 15 N respectively.

The application force is continuously applied to the deposited ceramic layer until it is perforated. From the time-force distribution (fig. 5a and b) a higher resistance of the layer deposited on the sample 2, especially the first layer deposited directly on the material, is observed, the breaking force increasing sharply in the last 4 s of loading (fig. 5b - interval 56 -60 s).

Figure 6 shows the SEM images of the metallic + ceramic coating surface after the scratch test performed for the two samples P1 (less roughness) and P2. Figure 6a and d show the whole scratch image in figure 6b and the deformed ceramic layer in the middle of the test and in figure 6c and f the area where the ceramic layer was pierced and the cast iron substrate was reached. The

Element	P1			P2		
	wt.%	at.%	Error %	wt.%	at.%	Error %
O	52.35	72.14	1.12	50.10	70.32	1.58
Al	28.49	23.28	0.58	28.38	23.61	0.76
Zr	16.66	4.02	0.61	18.01	4.43	0.72
Y	1.89	0.46	0.12	1.91	0.48	0.13
Hf	0.59	0.07	0.05	0.70	0.08	0.05

Table 1
CHEMICAL COMPOSITION OF DEPOSITS ON SAMPLES P1 (R_a: 2.47μm) AND P2 (R_a: 4.25μm)

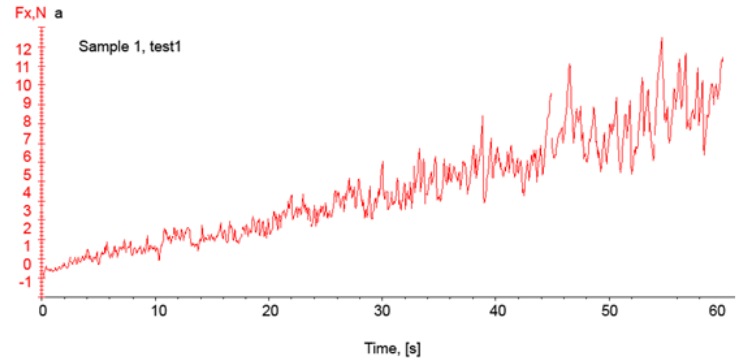

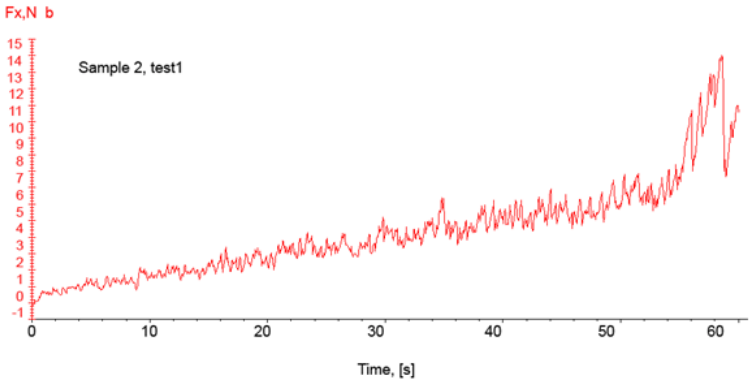

Fig. 5. Behavior of complex ceramic thin layers during scratching: a. test on sample P1; b. Test on sample P2

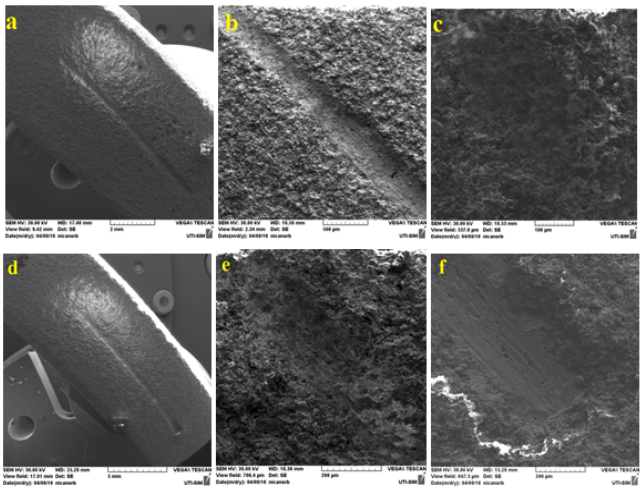

Fig. 6. SEM images of the surface of the ceramic after the scratch test: sample P1; d.-f. sample P2

scratch test is about 12 mm (fig. 6a and d), advancing at a rate of 0.2 mm/s.

Figure 6c and f show the penetration area in the material at 12 N and 15 N forces, this process being approximately 0.5 mm apart. At the edges of the material deposited in the penetration zone, no macro-cracks or exfoliations of the material are observed since the deposited layer is compact and brittle which leads to a fragile layer breakage without visible elastic manifestations of the ceramic material. The trace left by the tip of the test equipment does not show adjacent cracks, pores or exfoliations but only areas of deformed material, (fig. 6b and e).

Surface traces left in the deposited layer were investigated by profilemetry in three zones on their 12 mm length, namely at the beginning, middle and at the end of the stress when the deposited layer was penetrated. Twelve profile shapes corresponding to the two samples P1 and P2 and two scratches on each sample were made. Figure 7 shows the results obtained from the profiles for each sample with details of the surface condition for each test trace.

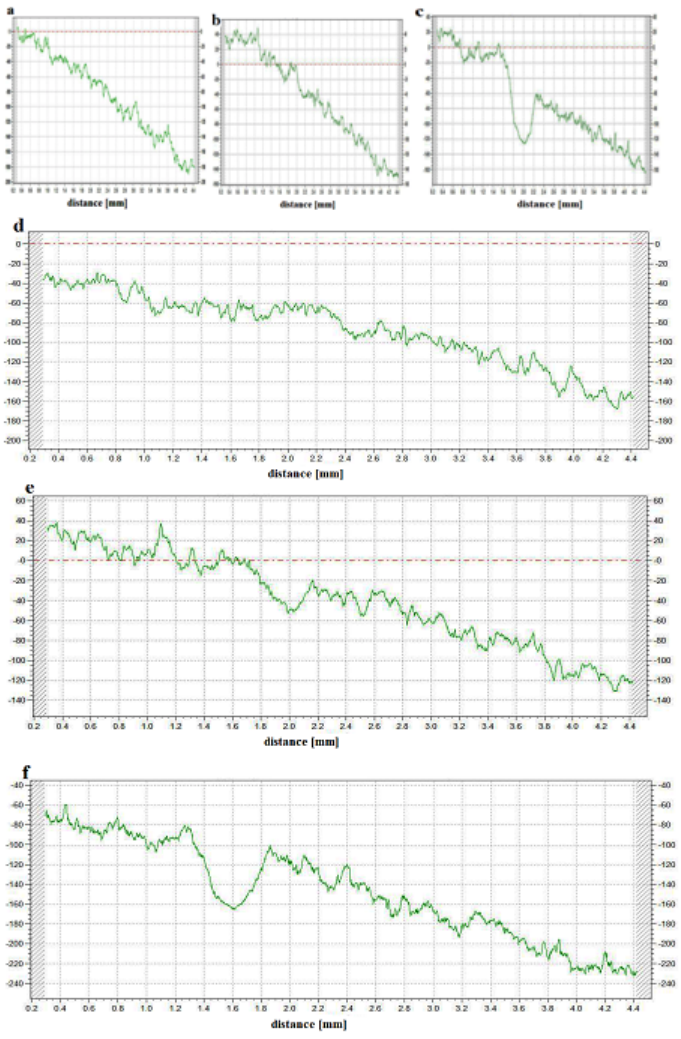

Fig. 7. Profileometries made on samples P1 and P2 for the two scratch marks: at the beginning of the trace - a and d; in the middle of the line - b and e; at the end of the trace - c and f

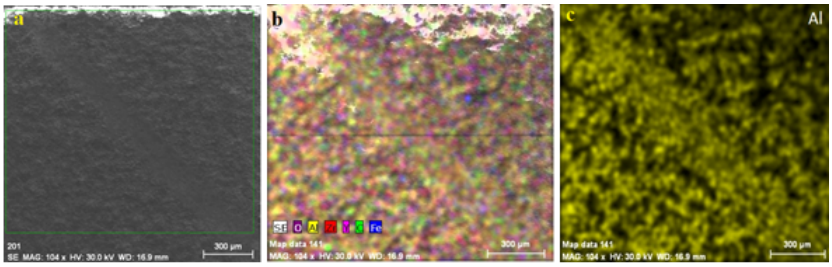

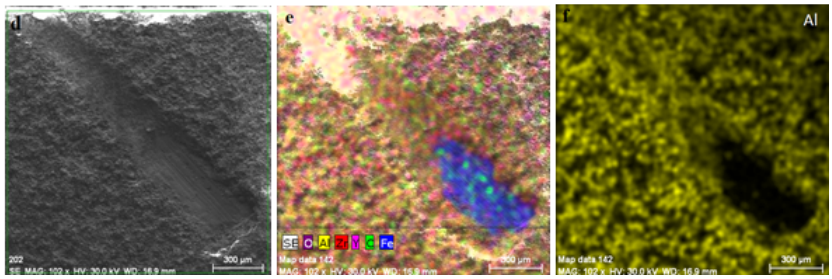

Fig. 8. Distribution of the elements O, Al, Zr, Y and Fe: at the beggining of the scratch, a-c; at the end of the scratch, d-f.

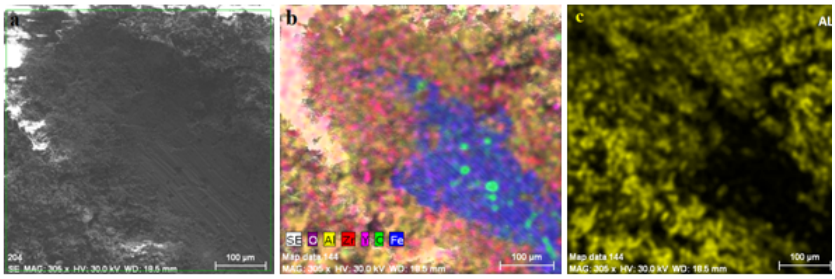

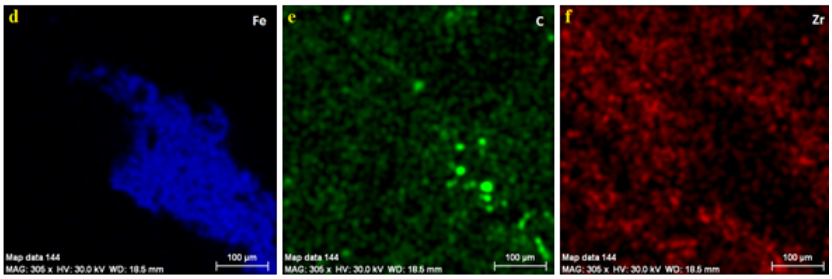

Fig. 9. Distribution of Al, Zr, C and Fe elements at the end of the scratch, where the layer was pierced

Profile geometries were made transversely to scratches. The deposited layer is relatively rough and a depth variation can be seen only at the end of the adhesion test, (fig. 7c and f), where the penetrator pierced the ceramic layer and reached the substrate. It is observed from the profile geometry that the depth of the layer is about 60 μm.

Figures 8 and 9 show the distributions of elements deposited on the deposited layer or the substrate after the scratch tests for sample P1 or P2 sample. Figure 8 shows the distribution of the O, Al, Zr, Y and Fe elements at the scratch start, figure 8a-c and figure 8d-f at the end of the scratch. For the first part of the scratch mark, no chemical changes or exfoliations can be observed, it is only a slight contour of the aluminum on the surface (fig. 8c). For the end of the scratch, figure 8d-f, the substrate is touched, figure 8e in which the iron element and locally the carbon element appears, and figure 8f in which the deposited layer represented in this distribution by the aluminum completely disappears.

From figure 8b, the local appearance of iron is observed on the edge of the scratch, due to the partial exfoliation of the ceramic layer on very small surfaces due to the very brittle nature of the ceramic layer and the influence of the external force. It can also be appreciated that the ceramic layer did not adhere perfectly to the material. Figure 9 shows the distribution of the O, Al, Zr, Y and Fe, C elements at the end of the P2 scratch, where the ceramic layer was pierced.

From the total distribution but also from the individual elements of the elements we can see the area where the layer was perfored in this case, sample P2, there is a final deterioration of the prolonged layer compared to the sudden layer of the sample 1, which can be put on the better adhesion between the substrate and the substrate as a function of the roughness of the substrate.

Conclusions

Ceramic superficial layers (made of complex oxides of aluminum, zirconium and yttrium oxide) were obtained by plasma deposition at a powder temperature of 12000°C on FC 250 cast iron substrates. The layers were obtained by five successive passes and - performed 60 μm thicknesses on differently processed surface samples and different roughness (0.34; 2.47 and 4.25 μm). As a result of these tests, compact layers were observed on experimental samples with micro-cracks at the surface due to the thermal gradient that occurs during the deposition procedure. From the chemical analysis of the obtained ceramic layers, a very good reproducibility of the deposition method has been observed even if it has already established industrial applications.

From the adhesion point of view, the highest roughness test, ie P2, resisted the most until the layer was perfored by approximately 15 N compared to the roughness of less than 12 N. The scratch marks did not show cracks, pores or exfoliations adjacent.

References

1. SELLAMI, A., KCHAOU, M., ELLEUCH, R., CRISTOL, A.L., DESPLANQUES, Y., Mater. Des., **59**, 2014, p. 84.
2. SANDU, A.V., CIOMAGA, A., NEMTOI, C., BEJINARIU, C., SANDU, I., Journal of Optoelectronics and Advanced Materials, **14**, no. 7-8, 2012, p. 704.
3. NEJNERU, C., VIZUREANU, P., SANDU, A.V., GRECU, A., CIMPOESU, N., Rev. Chim. (Bucharest), **65**, no. 2, 2014, p. 194.
4. FILIP, P., WEISS, Z., RAFAJA, D., Wear, **252**, 2002, pp. 189.
5. GARG, B.D., CADLE, S.H., MULAWA, P.A., GROBLICKI, P.J., LAROO, C., PARR, G.A., Environ. Sci. Technol., **34**, 2000, p. 4463.
6. SANDERS, P.G., XU, N., DALKA, T.M., MARICQ, M.M., Environ. Sci. Technol., **37**, 2003, p. 4060.
7. PAPADATU, C.P., SANDU, A.V., BORDEI, M., SANDU, I.G., Rev. Chim. (Bucharest), **68,** no. 4, 2017, p. 675.
8. PAPADATU, C.P., Experimental studies regarding wear processes through dry friction of the superficial layer for an unconventional treated steel, Edited by: RIPA, M., RIPEANU, R.G., CICONE, T., Conference: 13th International Conference on Tribology (ROTRIB) Location: Galati, Romania Date: SEP 22-24, 2016, 13TH International Conference on Tribology (ROTRIB'16) Book Series: IOP Conference Series-Materials Science and Engineering, **174**, 2017, Article Number: UNSP 012014
9. BLAU, P.J., MEYER, H.M., Wear, **255**, 2003, pp. 1261–1269.
10. SANDU, A.V., BEJINARIU, C., NEMTOI, G., SANDU, I.G., VIZUREANU, P., IONITA, I. , BACIU, C., Rev. Chim. (Bucharest), **64,** no. 8, 2013, p. 825.
11. KRISTKOVA, M., FILIP, P., WEISS, Z., PETER, R., Polym. Degrad. Stabil., **84**, 2004, p. 49.
12. LI, D., LIU, L., ZHANG, Y., YE, C., REN, X., YANG, Y., YANG, Q., Mater. Des. **30**, 2009, p. 340.
13. NICA, P.E., AGOP, M., GURLUI, S., BEJINARIU, C., FOCSA, C., Jpn. J. Appl. Phys., **51**, 2012, 106102.
14. WEISS, Z., CRELLING, J.C., MARTYNKOVA, G.S., VALASKOVA, M., FILIP, P., Carbon, **44**, 2006, p. 792.
15. BACAITA, E.S., BEJINARIU, C., ZOLTAN, B., PEPTU, C., ANDREI, G., POPA, M., MAGOP, D., AGOP, M., J. Appl. Math., 2012, 653720.
16. BUZEA, C.G., BEJINARIU, C., BORIS, C., VIZUREANU, P., AGOP, M., Int. J. Nonlinear Sci. Numer. Simul., **10**, 2009, p. 1399.
17. PAPADATU, C.P., SANDU, I.G., BORDEI, M., NABIALEK, M., SANDU, A.V., Mat. Plast., **53,** no. 4, 2016, p. 771.
18. PAPADATU, C.P., SANDU, A.V., BORDEI, M., SANDU, I.G., Rev. Chim. (Bucharest), **67,** no. 11, 2016, p. 2306.
19. PAPADATU, C.P., SANDU, A.V., BORDEI, M., SANDU, I.G., Rev. Chim. (Bucharest), **68,** no. 10, 2017, p. 2329.
20. SOFRONI, L., Elaborarea si turnarea aliajelor, EDP Bucuresti, 1975.
21. TANG, X.H., CHUNG, R., PANG, C.J., LI, D.Y., HINCKLEY , B., DOLMAN, K., Wear, **271**, 2011, p. 1426.
22. BEJINARIU, C., SANDU, A.V., BACIU, C., SANDU, I. , TOMA, S.L., SANDU, I.G., Rev. Chim. (Bucharest), **61**, no. 10, 2010, p. 961.
23. CIMPOESU, R. H., POMPILIAN, G. O., BACIU, C., CIMPOESU, N., NEJNERU, C., AGOP, M., GURLUI, S., FOCSA, C., Optoelectron. Adv. Mater.-Rapid Commun., **4**, 2010, p. 2148.
24. PINTILEI G.L., CRISMARU V.I., ABRUDEANU M., MUNTEANU C., LUCA D.; ISTRATE B., Applied Surface Science, **352**, 2015, p. 169.
25. SANDU, A.V., CIOMAGA, A. NEMTOI, G., ABDULLAH, M.M.A., SANDU, I., Instrumentation Science & Technology, **43**, no. 5, 2015, p. 545.
26. FLOREA, C.D., BEJINARIU, C., CARCEA, I. , PALEU, V., CHICET, D.L., CIMPOE^{a}U, N., Key Engineering Materials, **660**, 2015, p. 97.
27. NEDEFF, V., BEJENARIU, C., LAZAR, G., AGOP, M., Powder Technol., **235**, 2013, p. 685.
28. SANDU, A. V., CIOMAGA, A., NEMTOI, G., BEJINARIU, C., SANDU, I. , Microsc. Res. Tech., **75**, no. 12, 2012, p. 1711.
29. TOMA, S. L., BEJINARIU, C., BACIU, R., RADU, S., Surf. Coat. Technol., **220**, 2013, p. 266.
30. FLOREA, C., BEJINARIU, C., MUNTEANU, C., CIMPOESU, N., Preliminary Results on Complex Ceramic Layers Deposition by Atmospheric Plasma Spraying. in Advanced Materials Engineering and Technology V, Amer. Inst. Physics: Melville, **1835**, 2017, 020053.
31. CALIN, M.A., KHENOUSSI, N., SCHACHER, L., ADOLPHE, D., MANEA, L.R., GRADINARU, I., ZETU, I. , STRATULAT, S., Mat. Plast. **50**, no. 4, 2013, p. 257.
32. TEODORESCU, M., SCHACHER, L., ADOLPHE, D., GRADINARU, I., ZETU, I. , STRATULAT, S., Mat. Plast. **50**, no. 3, 2013, p. 225.
33. BALTATU, M.S., VIZUREANU, P., CIMPOESU, R., ABDULLAH, M.M.A.B., SANDU, A.V., Rev. Chim. (Bucharest), **67**, no. 10, 2016, p. 2100.
34. BUJOREANU, C., BENCHEA, M., Experimental study on HVAC sound parameters. IOP Publishing Ltd: Bristol , **147**, 2016, 012051.

Manuscript received: 15.04.2017